Preparation and Characterization of PMMA Nanocomposites Based on ZnO-NPs for Antibacterial Packaging Applications

Ahmed Youssef[1], Islam EL-Nagar[1], Alaa El-Torky[2], Abou El-Fettouh Abd El-Hakim[1]
[1]Packaging Materials Department, National Research Centre
El-buhoth Street 33, 12622, Dokki, Cairo, Egypt
amyoussef27@yahoo.com; am.abdel-wahab@nrc.sci.eg
[2] Chemistry Department, Faculty of Science
Zagazig University, Zagazig, Egypt

Abstract - This study aims to synthesis and characterize of poly (methyl methacrylate) nanocomposites that based on methyl methacrylate monomer (MMA) and zinc oxide nanoparticles (ZnO-NPs), namely PMMA/ZnO nanocomposite via in-situ emulsion polymerization of MMA monomer using potassium persulphate (PPS) as initiator. ZnO-NPs were firstly prepared through hydrothermal method. The prepared ZnO-NPs were investigated by X-Ray diffraction pattern (XRD), Fourier transform infrared (FT-IR) and transmission electron microscope (TEM). PMMA/ZnO nanocomposites were prepared via emulsion polymerization using different concentrations of ZnO-NPs (2%, 4%, 8% and 12%) based on monomer concentration. Furthermore, PMMA/ZnO nanocomposites were studied using FT-IR, TEM, XRD, UV/Vis spectroscopy and thermal gravimetric analysis (TGA). The fabricated poly (methyl methacrylate) nanocomposites display good morphological, thermal properties and antibacterial activity than pure PMMA. Additionally, the PMMA nanocomposites display respectable antimicrobial activity against gram positive (*Staphylococcus aureus*) bacteria, gram negative (*Pseudomonas aeruginosa)* bacteria and yeast (*Candida albicans*). Additionally, the PMMA nanocomposites can be used as good materials for antibacterial packaging applications.

Keywords: PMMA, Nanocomposite, ZnO-NPs, Antibacterial activity, Packaging applications.

1. Introduction

Polymer nanocomposites consider most attractive class of materials for a new performance, attributable to their amazing properties via consuming a low to high fillers loading in nanoform [1, 2]. Addition of inorganic nanoparticles (NPs) to polymers matrix may present precise functionalities (antibacterial, catalytic activity, etc.) also develop the mechanical, electrical properties, thermal stability, and fire retardant [3, 4]. Also, nanotechnology is recently considering one of the most important areas for packaging technological development in the 21st century [5]. Furthermore, nanocomposites materials become a development area of recent research, which cover wide range of systems with potentially novel material properties [6]. PMMA has great interest and many advantages as a result of its individual properties such as Lower optical absorption due to its high transparency in the visible region, low refractive index, rigid, hard, thermal capacity, electrical performance, good mechanical properties and simple synthesis process [7].

Furthermore, PMMA is frequently used as an alternate to materials such as glass. Though, pure PMMA displays some drawbacks, for instance low thermal stability, which bounds PMMA from high-temperature applications. Poly (methyl methacrylate) transfers UV light; therefore, producers frequently making UV layers on PMMA to overwhelm this lack [8]. Inorganic fillers in nanoform were added to the polymer matrix, including PMMA/clay nanocomposites [9, 10], PMMA/SiO$_2$ nanocomposites [11, 12] as well as PS/TiO$_2$ nanocomposites [13, 14]. PMMA/ZnO nanocomposites were widely examined in the literature [15, 16]. Correspondingly, PMMA can be used to design everything [17, 18] due to its hydrolysis resistance and good resistance to outdoor weather and thermoplastic properties.

In last years, ZnO nanoparticles have got worldwide attraction as a result of its individual properties [19, 20] such as its chemical stability, antibacterial property, catalytic activity and less toxicity [21], high refractive index, wide band gap and ultraviolet absorption. It can be determined these characteristics synergistically through nanohybrides preparation. In addition, ZnO-NPs have a high surface energy since it is easily aggregated through the process of mixed configuration. Besides, the regular dispersion of inorganic filler with host materials is greatly eligible to achieve the preferred properties of hybrid materials [22].Owing to this fact; it is suggested to modify the surface of zinc oxide nanoparticles to adjust dispersion

ability [23]. Literature review shows that modification of nanoparticles by polymer grafting is appropriate and satisfactory technique [24, 25]. Moreover, several studies were intensive on PMMA/ZnO nanocomposites and its thermal degradation behaviour due to the properties and applications of PMMA in medicine, chromatography, as well as optics instruments [26]. The combination of ZnO-NPs with PMMA matrix is thought to enhance the optical properties of the PMMA.

In the current study we emphases on the influence of addition of ZnO-NPs to PMMA in in-situ emulsion polymerization. Initially, the hydrothermal method was used to fabricate ZnO-NPs. The prepared ZnO-NPs as well as PMMA/ZnO nanocomposites were examined via transmission electron microscopy (SEM), scanning electron microscopy (TEM), thermal gravimetrical analysis (TGA), UV–Vis spectroscopy, and the antimicrobial activity.

2.1. Materials

Methyl Methacrylate was purchased from Sigma Aldrich, also potassium persulfate as initiator (PPS, $K_2S_2O_8$, Reanal, Hungary) was used to prepare the polymer samples. Sodium dodecyl sulphate(SDS) was used as a cationic surfactant. Zinc-acetate (puriss, Reanal, Hungary) (Zn $(CH_3COO)_2$. $2H_2O$) was used to prepare ZnO nanoparticles. Sodium hydroxide (NaOH) was purchased from Acros. Distilled water was used in all preparation procedures. All chemicals and reagents are of analytical grade and used without any further purification.

2.2. Preparation of ZnO nanoparticles

ZnO nanoparticle was prepared in alcoholic medium by the reaction of zinc acetate and a base (NaOH). In this study, 3.942 g zinc acetate and 1.44 g NaOH were dissolved in 1L ethanol and refluxed at 60° C for 1 h. The acetate group reacted with (NaOH) and converted zinc acetate into zinc oxide. The prepared ZnO-NPs that is dispersed in alcohol medium was transparent and clear and was capable of maintaining stable for at least 2 weeks. After reaction, the zinc oxide that was dispersed in ethanol was mixed with DI-water for purification. ZnO nanoparticles were then separated from the dispersion supernatant by centrifugation at 7000 rpm for 5 min repeatedly. Finally the ZnO nanoparticles were dispersed in DI-water to obtain ZnO-NPs water dispersion. TEM result indicated that the size of ZnO-NPs were about 5-20 nm, as shown in (Fig. 3).

2.3. Preparation of PMMA/ZnO nanocomposites

Poly (methyl methacrylate) nanocomposites were prepared via in-situ emulsion polymerization based on ZnO nanoparticles, which were first dispersed into deionized water at different loadings (2%, 4%, 8% and 12%) based on monomer concentration), to employment as seeds for emulsion polymerization of methyl methacrylate monomer in the presence of (SDS) as a cationic surfactant and potassium persulphate (PPS) as an initiator as shown in Table 1. The dispersion was prepared, in a 250 ml flask, by mixing ZnO-NPs and SDS as a surfactant with 80 ml deionized water, and then the mixture was sonicated for 30min. The desired amount of methyl methacrylate (10 ml) was added to the mixture under sonicated then dissolve a suitable amount of PPS as initiator in 10ml deionized water and added drop by drop. The flask was immersed in a water bath, heated to 80ºC, the polymerization was then started while kept under magnetic stirring (700 rpm).The emulation was precipitated and dried in an electric oven at 60ºC (Thermo Scientific Heraeus, USA).

Table 1: the recipe of the emulsion polymerization of MMA using different concentrations of ZnO-NPs in presences of PPS as initiator and SDS as emulsifier at 80°C.

Samples	MMA	PPS	ZnO-NPs	Temperature	SDS
Pure PMMA	10 g	0.1 g	0.0	80°C	0.2 g
PMMA/ZnO nanocomposite	10 g	0.1g	0.2	80°C	0.2 g
PMMA/ZnO nanocomposite	10 g	0.1g	0.4g	80°C	0.2 g
PMMA/ZnO nanocomposite	10 g	0.1g	0.8g	80°C	0.2 g
PMMA/ZnO nanocomposite	10 g	0.1g	1.2g	80°C	0.2 g

2.4. Characterization of ZnO-NPs and PMMA/ZnO nanocomposite

Powder XRD was performed on a Rigaku, Miniflex X-ray diffractometer ME 14848DO4 with CuKa radiation source (k¼1.5418 A˚) (Japan). The d-spacing was calculated via Bragg's equation. PMMA/ZnO nanocomposites samples used for XRD were glued to a glass slide by separating the samples homogenously on it. The samples were placed in a vertical configuration (transmission) for the collection of XRD data. The microstructure of the samples was examined using JEOL JEM-1230 transmission electron microscope (TEM) (JEOL JEM-1230, Tokyo, Japan) with acceleration voltage of 80 kV. The microscopy probes of the nanocomposite samples were prepared by adding a small drop of the water dispersions onto a Lacey carbon film-coated copper grid, then allowing them to dry in air. Also, scanning electron microscope (SEM), Tescan VEGA-II, USA, operated at 20 kV, was used for examining the nanoparticles morphologies and surface characters of the resulting nanocomposites. The thermal behavior was studied using a Perkin Elmer thermal gravimetric analyzer (TGA) operated under nitrogen atmosphere at a heat in grate of 10°C/min.

2.5. Evaluation of Antimicrobial Activity

The antimicrobial activities of the prepared nanomaterials and its nanocomposites were studied using disc agar plate method was employed to evaluate the antimicrobial activity of the prepared nanocomposites [3, 21]. The antimicrobial activities of 0.5 cm diameter of nanocomposites disc (5 mm) were placed on agar plates seeded with test microbes and incubated for 24 hrs at the appropriate temperature of each test organism. PMMA nanocomposites samples were tested against four different microbial strains, i.e., *Staphylococcus aureus* ATCC6538-P (G+ve bacteria), *Pseudomonas aeruginosa* ATCC 27853 (G-ve bacteria), *Candida albicans* ATCC 10231 (yeast). The bacterial and yeast test microbes were grown on a nutrient agar medium (DSMZ1) of the following components (g/l): Peptone (5.0), Meat extract (3.0), Agar (20.0), distilled water (1000.0 ml) and the pH to 7.0. On the other hand, the fungal test microbe was cultivated on Czapek-Dox medium (DSMZ130) of the following ingredients (g/l): Sucrose (30.00), $NaNO_3$ (3.0), $MgSO_4$ x 7 H_2O (0.50), KCl (0.50), $FeSO_4$ x 7 H_2O (0.01), K_2HPO_4 (1.0), agar (18.0), distilled water (1000.0ml) and the pH was adjusted to 7.2. The culture of each test microbe was diluted by distilled water (sterilized) to about 107 - 108 cells/ml, then 1ml of each was used to inoculate 1L-Erlenmeyer flask containing 250 ml of solidified agar media then poured in Petri dishes (10cm diameter containing 25 ml). Discs (5 mm diameter) were placed on the surface of the agar plates previously inoculated with the test microbe and incubated for 24 hrs. for bacteria and yeast but for 48 hrs. The test microorganisms were obtained from the culture collection centre, Microbial Chemistry Department, National Research Centre, Egypt.

3. Result and Discussion
3.1. X-ray diffraction pattern of ZnO-NPs and PMMA/ZnO nanocomposites

Figure 1 represents the X-ray diffraction pattern (XRD) of PMMA, ZnO-NPs and PMMA/ZnO nanocomposites based on ZnO-NPs which added with different concentrations (2, 4, 8 and 12% ZnO-NPs). The ZnO-NPs was fabricated using hydrothermal method in this method ethanol was performances as a reaction medium. The X-ray diffraction pattern of the

obtained ZnO-NPs is shown in (**Fig. 1**) for 2θ diffraction angles between 10 and 80 displays most attributed peaks that related to the planes (100) at 2θ=31.76°, (002) at 2θ=34.44°, (101) at 2θ=36.25°, (102) at 2θ=47.42°, (110) at 2θ=56.57°, (103) at 2θ=62.86° in addition to (112) at 2θ=67.93°. The result get from XRD pattern demonstrated that the largest part of diffraction peaks consent with the stated JCPDS data and the manufacture of ZnO nanoparticles very similar to the packed hexagonal Wurtzite structure.
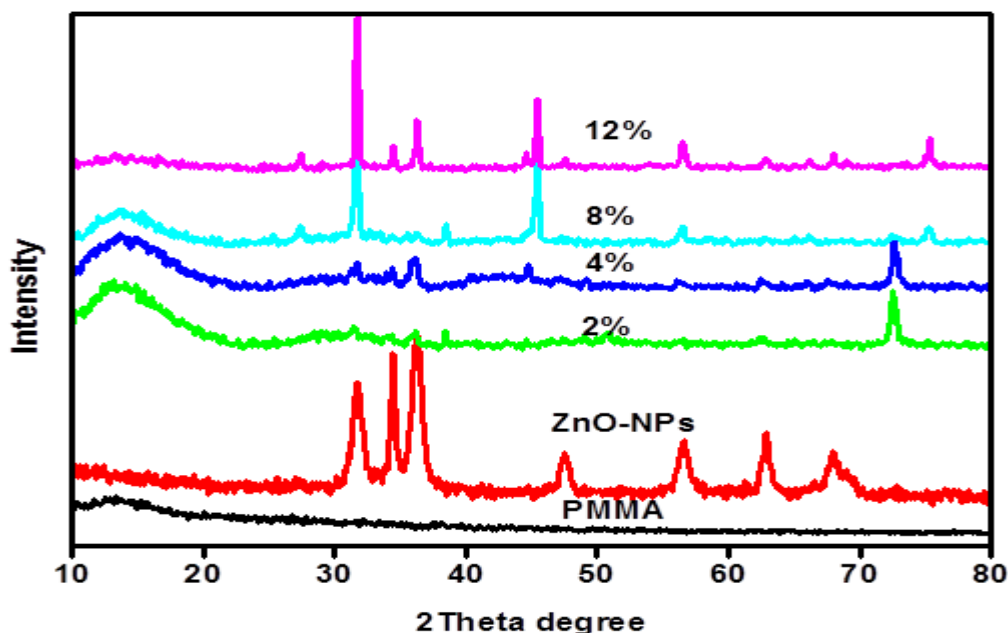
Fig. 1: XRD patterns for PMMA, ZnO-NPs and PMMA/ZnO nanocomposites loaded with 2% ,4% ,8% and 12 wt% ZnO-NPs.

While XRD pattern of PMMA display that there is no significant peak but there is peak at 2θ =13.5° that related to the crystalline polymer structure. Moreover, the XRD pattern of PMMA/ZnO nanocomposites loaded by different concentrations of ZnO-NPs (2%, 4%, 8%, and 12%) was illustrated in (**Fig. 1**) that exhibited the existence of ZnO-NPs into the polymer matrix in all ZnO-NPs loadings that confirmed the well formation of PMMA/ZnO-NPs nanocomposites. Additionally, the intensity of ZnO-NPs peaks in the PMMA nanocomposites was increased by increasing the loadings of ZnO-NPs in the polymer matrix.
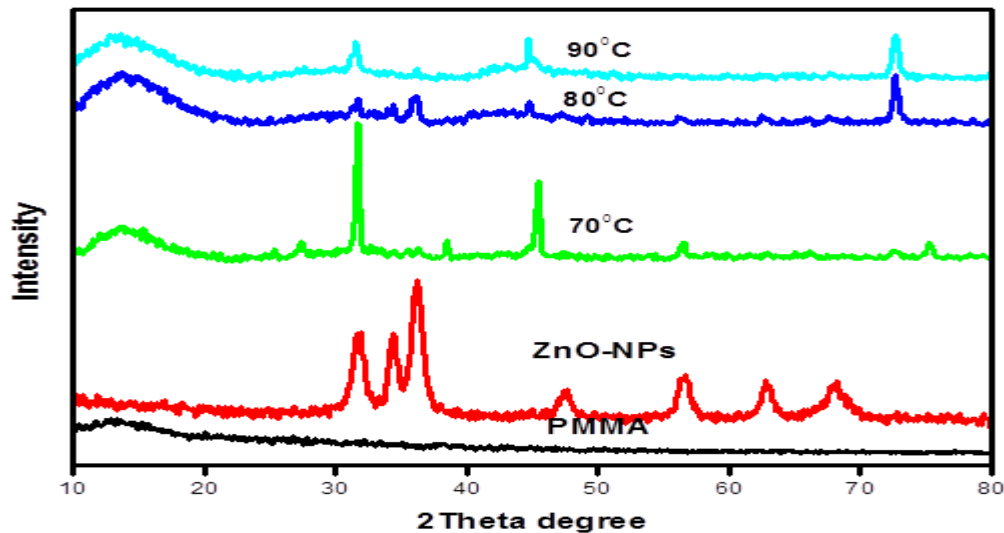
Fig. 2: XRD patterns for PMMA, ZnO-NPs and PMMA/ZnO nanocomposites at different reaction temperature (70˚C, 80˚C and 90˚C) and 4% of ZnO-NPs.

Figure 2 displayed that the X-ray diffraction pattern (XRD) of PMMA, ZnO-NPs and PMMA/ZnO nanocomposites based on ZnO-NPs at different reaction temperatures (70˚C, 80˚C and 90˚C)**.**. The PMMA/ZnO nanocomposites were fabricated using in-situ emulsion polymerization method. The X-ray diffraction pattern of the obtained PMMA nanocomposites at different reaction temperature is revealed in (**Fig. 2**) which demonstrated that the presence of (4 %, ZnO-NPs) into the PMMA matrix in all reaction temperatures that confirmed the well formation of PMMA/ZnO nanocomposites. Additionally, the intensity of ZnO-NPs peaks in the PMMA at reaction temperature (70˚C) was the best one among the other reaction temperatures (80˚C and 90˚C**)** into the PMMA nanocomposites matrix.

3.2. Morphological studies of PMMA/ZnO nanocomposites

The morphological properties of the prepared ZnO-NPs as well as PMMA/ZnO nanocomposites with different concentrations of ZnO-NPs were evaluated using TEM and SEM. The development of ZnO-NPs distribution is significant subsequently the good dispersion of ZnO-NPs that result in an essential enhancement in the properties of the fabricated PMMA/ZnO nanocomposites. **Fig. 3** symbolized the TEM photographs of the prepared ZnO-NPs as well as PMMA/ZnO nanocomposites. ZnO-NPs were synthesized via hydrothermal method used zinc acetate as precursor and high alkaline medium (0.5 M NaOH) at 150°C for 6 h in presences of absolute ethanol as a solvent, ZnO-NPs was formed in a single crystalline form. The result obtained from TEM image supports the manufacture of ZnO-NPs in nanostructured form, which is reputable agreement with XRD data (**Fig. 1**). The fabricated ZnO-NPs in the nanometer scale with an average size around10 nm were dispersed in PMMA/ZnO nanocomposites, which lead to well significance results on the various properties of the synthesized PMMA nanocomposites for example; thermal and antimicrobial properties.

Homogeneous dispersion of ZnO-NPs is preferred to avoid formation of crack creativities in the PMMA nanocomposites. In order to think about the influence of ZnO-NPs in the PMMA matrix loaded (2–12 wt %) on the distribution and the dispersion of the ZnO as nanofiller in the PMMA nanocomposites matrix, scanning electron microscope (SEM) was used to evaluate the dispersion of ZnO-NPs in the nanocomposite matrix.
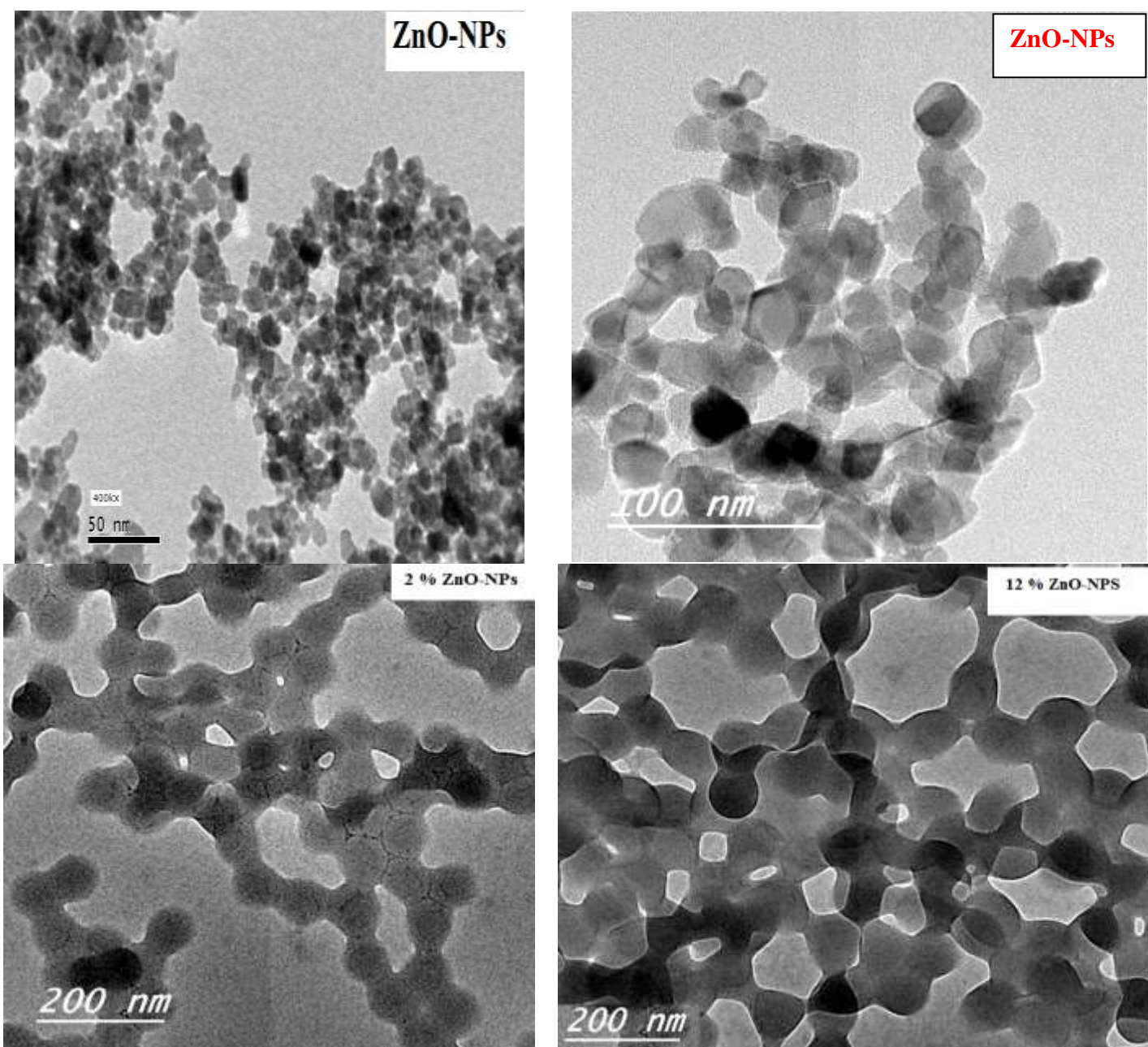
Fig. 3: TEM image of ZnO-NPs as well as PMMA/ZnO nanocomposites containing different concentrations of ZnO-NPs (2, and 12 %).
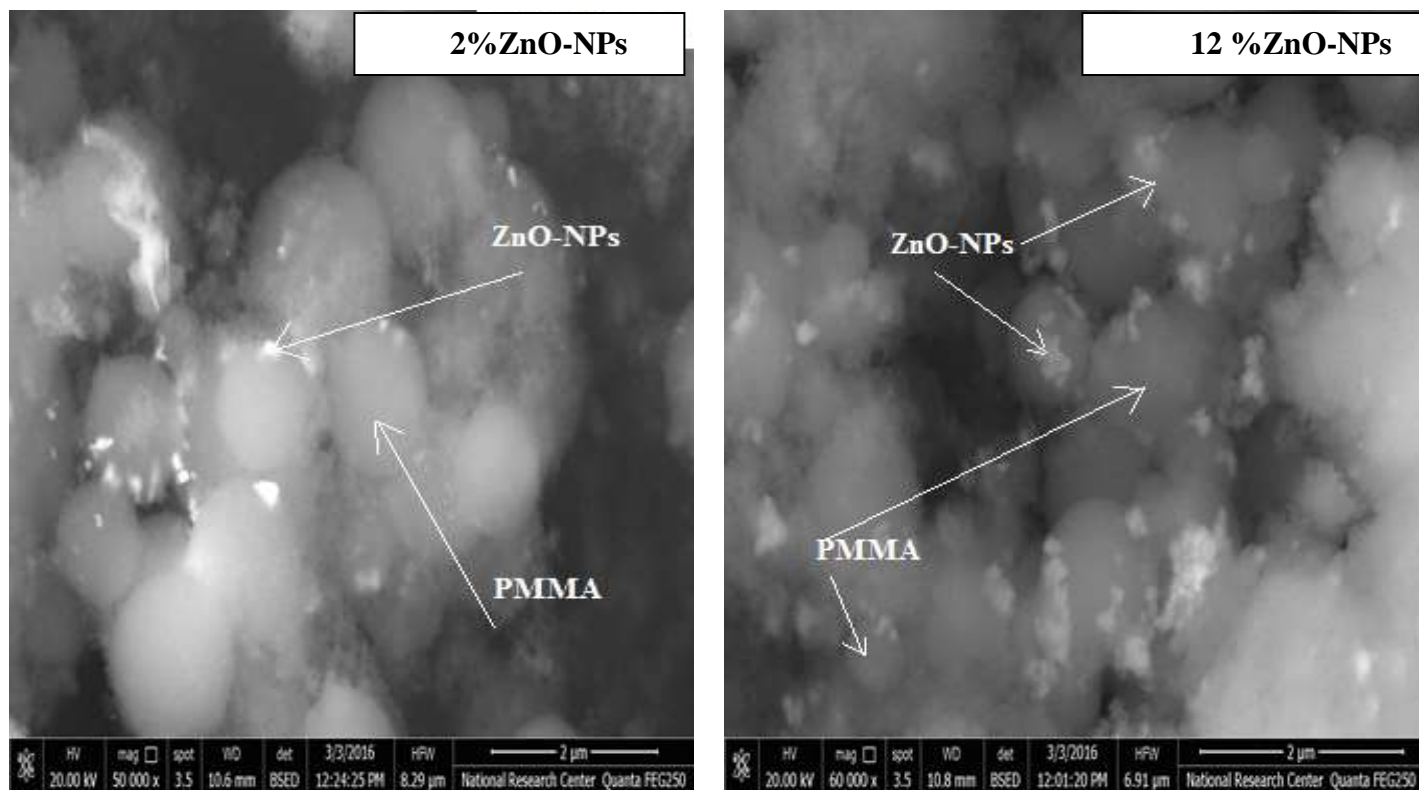
Fig. 4: SEM image of ZnO-NPs as well as PMMA/ZnO nanocomposites containing different concentrations of ZnO-NPs (2, and 12 %).

Figure 4 displays SEM images of the PMMA/ZnO nanocomposites prepared using in situ emulsion polymerization of MMA monomer with 2 and 12wt% ZnO NPs. The 2wt% PMMA/ZnO nanocomposites demonstrated well dispersion of the ZnO-NPs in PMMA matrix with small agglomeration. The bright phase presents the ZnO-NPs in uniform distribution when the amount of ZnO-NPs increases up to 12wt%. The agglomeration observed at 12wt% PMMA/ZnO nanocomposites offerings a poor dispersion of ZnO-NPs in the PMMA nanocomposites matrix.

3.3. UV-vis spectroscopy of the prepared PMMA/ZnO nanocomposites

The fabrication of metal nanoparticles can be recognized through the observation of the representative plasma on in UV/vis spectra. Also, the particle size of the fabricated nanoparticles plays a significant role in varying the whole properties of the new nanocomposite materials. Thus, the size of prepared ZnO-NPs considers very important for discovering the novel properties of the fabricated PMMA/ZnO nanocomposites.

UV-vis spectroscopy technique is extensively used to study the optical properties of the prepared nanoparticles. **Fig. 5** reveals the absorption spectrum of ZnO-NPs powder; it displays a strong absorption band at about 370 nm [27]. This evident that significant the sharp absorption of ZnO designates the monodispersed nature of the dispersion of the fabricated ZnO-NPs. Furthermore, **Fig. 5** displays the UV–Vis transmission and absorption spectra of PMMA, ZnO-NPs as well as PMMA/ZnO nanocomposites as a function of wavelength. Also, Fig.5 demonstrated the absorption maximum peak of the PMMA/ZnO nanocomposites which is shifted to greater wavelengths associated to the pure PMMA. The pure PMMA do not absorb UV light down to 300 nm in wavelength, while the PMMA/ZnO nanocomposites containing different concentrations of ZnO-NPs (2–12 wt%) as well as different reaction temperature absorb UV light at about 370-380 nm. The PMMA/ZnO nanocomposites absorption peaks are revealed at 370 nm corresponding to the exciting state in the ZnO

nanoparticles. The PMMA/ZnO nanocomposites containing 12% of ZnO-NPs reveal good UV-shielding efficiency. The increasing the ratio of ZnO-NPs in PMMA matrix, leading to more UV light is absorbed.
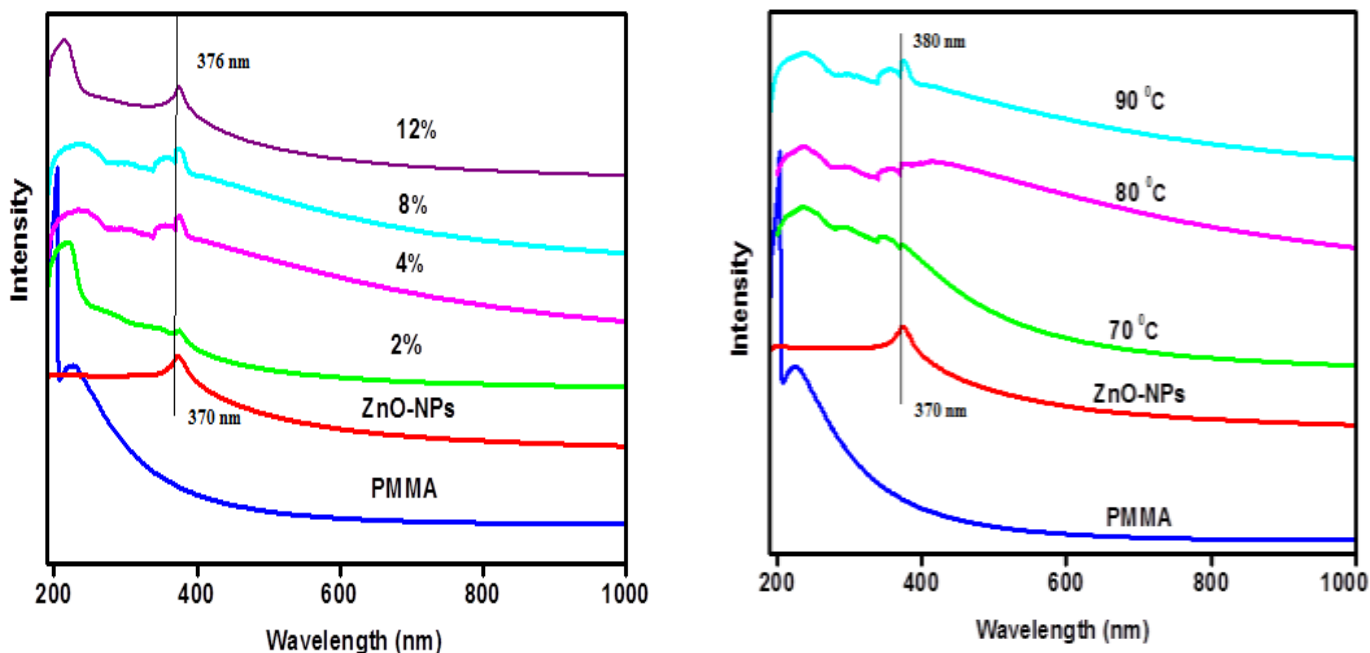

Fig. 5: UV-vis spectroscopy for pure PMMA, ZnO-NPs and PMMA/ZnO nanocomposites loaded with different concentration of ZnO-NPs (2%, 4%, 8% and 12 wt%) as well as at different reaction temperatures (70ºC, 80ºC and 90ºC).

3.4. FT-IR spectroscopy of the prepared PMMA/ZnO nanocomposites

FT-IR spectroscopy was used to detect the possible interactions that may be done by mixing PMMA with ZnO-NPs to form PMMA/ZnO nanocomposites. **Fig. 6** showed that the FT-IR spectra of PMMA, ZnO-NPs and PMMA/ZnO nanocomposites loaded with different concentrations of ZnO-NPs (2, 4, 8 and 12 wt%). The FT-IR spectrum of pure PMMA illustrate the absorption bands at 3004 and 2960 cm^{-1} that related to CH_2 stretching, and the bands at 1449 and 750 cm^{-1} related to the rocking and bending vibration of CH_2, correspondingly. The OH stretching show absorption peak at 3442 cm^{-1} .Moreover, stretching vibration of C=O of pure PMMA show characteristic absorption band at 1734 cm^{-1}.

FT-IR spectra were carried out with the intention of determines the clarity and nature of the ZnO nanoparticles. Metal oxides normally provide absorption bands in fingerprint region below 1000 cm^{-1} rising from inter-atomic vibrations. For ZnO-NPs the peak detected at 3450 and 1120 cm^{-1} are might be because of O-H stretching and deformation, individually allocated to the H_2O adsorption on the Zn surface. The bands at 1632, 615 cm^{-1} are matching to ZnO-NPs stretching and distortion vibration, respectively. Once the polymerization process happened and PMMA/ZnO nanocomposites were formed, all characteristics bands of PMMA and ZnO-NPs appears at all different loading of ZnO-NPs in the prepared PMMA/ZnO nanocomposites as shown in (**Fig. 6**).
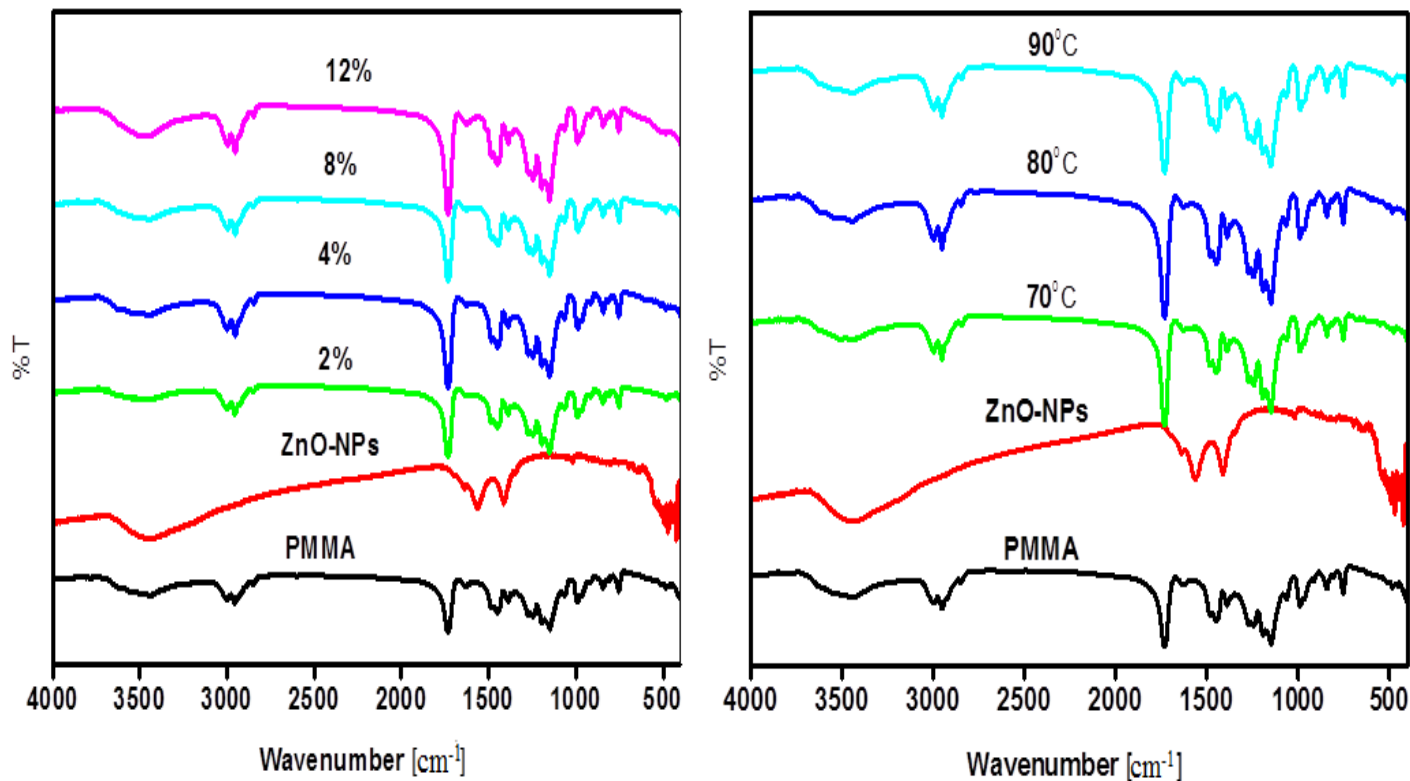
Fig. 6: FT-IR spectra for PMMA, ZnO-NPs and PMMA/ZnO nanocomposites at different concentrations of ZnO-NPs (2%, 4%, 8% and 12 wt%) as well as at different reaction temperatures (70ºC, 80ºC and 90ºC).

3.5. Thermal stability of the prepared PMMA/ZnO nanocomposites

The thermal properties of the fabricated PMMA/ZnO nanocomposite materials are very necessary and reflected the greatest significant characteristic of the key studies for different applications particularly in packaging of food products. Therefore, TGA is essential for creation and thermal stability of the prepared PMMA/ZnO nanocomposites which displayed in (**Fig.7**). **Figure 7** displays TGA of pure PMMA as well as PMMA/ZnO nanocomposites with various loadings of ZnO-NPs. The pure PMMA was obtainable via three main steps of thermal degradation. The first step was between T= 102 and 230ºC, weight loss of around 8wt% was ascribed to the vaporization of remaining solvent [28], and perhaps, a depolymerization stage was started at weak head-to-head links rising from chain termination through combining of vinylidene chain ends which outcome from disproportionation [29]. The second step was located among 235 and 410ºC. Furthermore, adding of ZnO-NPs into PMMA matrix enriches the thermal stability of the prepared PMMA/ZnO nanocomposites as shown in (**Fig. 7**). A remarkable improvement was detected at greater ZnO-NPs loadings when the highest thermal degradation peak rises by approximately 20 K associated to the main peak of pure PMMA. Correspondingly, the development of PMMA/ZnO-NPs nanocomposites thermal stability with rising the content of ZnO-NPs may be credited the morphological, thermal properties and antibacterial activity of PMMA/ZnO nanocomposites which open great view points for the applications of PMMA/ZnO nanocomposites in different fields.
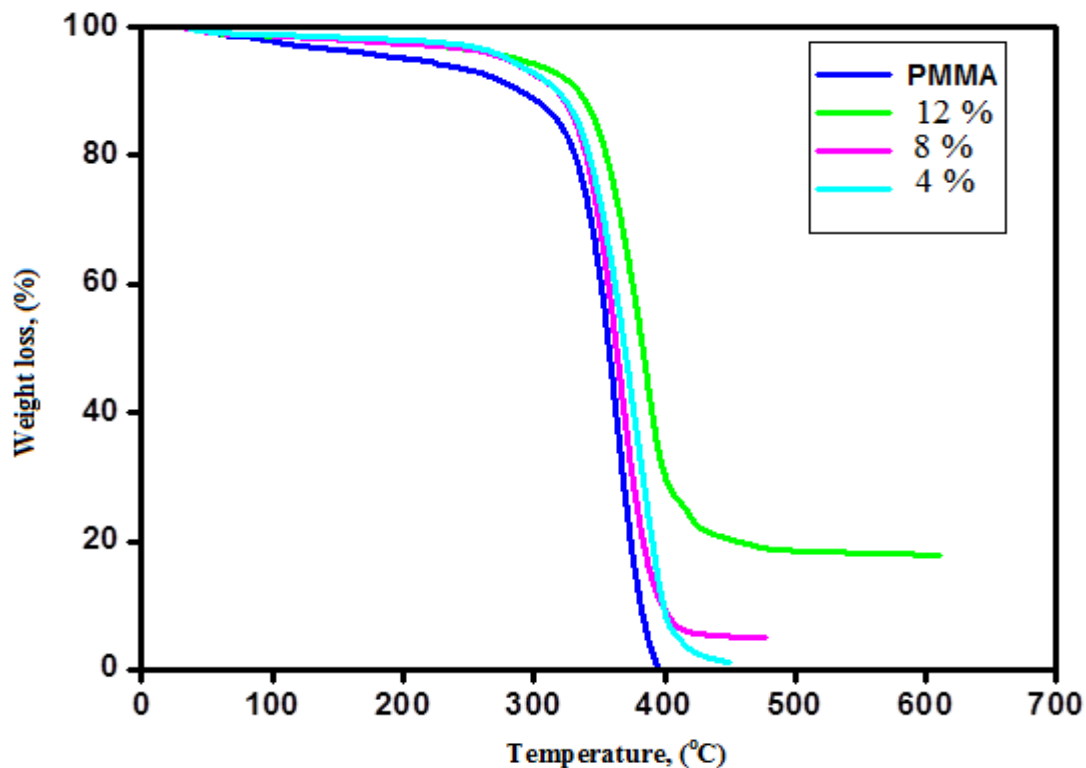
Fig. 7: Thermal gravimetric curves of PMMA as well as the PMMA/ZnO nanocomposites with different concentrations of ZnO-NPs, (4, 8 and 12%).

3.6. The antimicrobial activity of PMMA/ZnO nanocomposites

The antimicrobial activity of the fabricated PMMA/ZnO nanocomposites was carried out through agar plate method to determine the zone of inhibition of the synthesized PMMA nanocomposite films. Additionally, these films were examined against G^{+ve} (*Staphylococcus aureus*), G-^{ve} (*Pseudomonas aeruginosa*) bacteria as well as yeast (*Candida albicans*).The antimicrobial activities of the fabricated PMMA/ZnO nanocomposites against the bacteria and yeast were evaluated as shown in (**Fig.8**).

Figure 8 was displaying a significant increasing in the zone of inhibition by increasing the content of ZnO-NPs in the prepared PMMA/ZnO nanocomposites films. Furthermore, the strong inhibition zones of fabricated PMMA/ZnO nanocomposites films contrary to demonstrative strains of *Staphylococcus aureus* (G^{+ve}) and *Pseudomonas aeruginosa* (G-^{ve}) bacteria did not revealed an significant modification with increasing the concentrations of ZnO-NPs in case of the prepared nanocomposite films containing low loadings of ZnO-NPs as displayed in Figure 6. The inhibition zone was increased by increasing the ratios of ZnO-NPs in the PMMA matrix. It is predictable that the inhibitory influence of ZnO-NPs in contradiction of microorganisms up till now is not completely examined. It has been assumed that DNA misses its duplication ability and cellular proteins come to be deactivated.
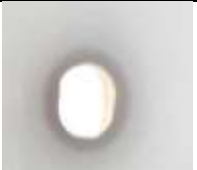
Samples	ZnO-NPs, %	*Staphylococcus aureus*	*Pseudomonas aeruginosa*	*Candidia albicans*
PMMA/ZnO nanocomposites	2%			
PMMA/ZnO nanocomposites	4%			
PMMA/ZnO nanocomposites	8%			
PMMA/ZnO nanocomposites	12%			

Fig. 8: The antimicrobial activity of the PMMA/ZnO nanocomposite against gram positive (*Staphylococcus aureus*), gram negative (*Pseudomonas aeruginosa*) bacteria and yeast (*Candida albicans*).

4. Conclusions

In current work we studied the dispersion of inorganic nanoparticles such as ZnO-NPs in a polymeric matrix (PMMA). Firstly, ZnO-NPs was prepared successfully via hydrothermal method, then added to PMMA matrix with different ZnO-NPs content (2–12 wt%) and study its influence on the morphological, thermal and antimicrobial properties of the fabricated PMMA nanocomposites. The optical properties of the prepared PMMA nanocomposites display transparent films at low concentration of ZnO-NPs. Also, rising in ZnO-NPs concentrations in the PMMA nanocomposites films improves the thermal stability of the fabricated PMMA/ZnO nanocomposites together with UV-shielding ability. PMMA nanocomposites containing ZnO-NPs display good antimicrobial activity against G^{+ve} (*Staphylococcus aureus*), G^{-ve} (*Pseudomonas aeruginosa*) bacteria as well as yeast (*Candidia albicans)*. Moreover, the improvement in thermal and optical properties of PMMA/ZnO nanocomposites along with its antimicrobial activity open huge probabilities for utilizing PMMA/ZnO-NPs nanocomposites in various applications such as (optical fields, solar energy and packaging applications).

References

[1]   A. M. Youssef. M. E. El-Naggar. F. M. Malhat, H. M. El Sharkawi, "Efficient removal of pesticides and heavy metals from wastewater and the antimicrobial activity of f-MWCNTs/PVA nanocomposite film," *J. Clean Product*., vol. 206, no. 1, pp. 315-325, 2019.

[2]   A. M. Youssef, S. M. El- Sayed, "Bionanocomposites materials for food packaging applications: Concepts and future Outlook," *Carbohyd. Polym.*, vol. 193, pp. 19–27, 2018.

[3]   A. M. Youssef, S. M. El-Sayed, H S. El-Sayed, H. H. Salama, F. M. Assem, M. H. Abd El-Salam, "Novel bionanocomposite materials used for packaging skimmed milk acid coagulated cheese (Karish)," *International Journal of Biological Macromolecules*, vol. 115, pp. 1002–1011, 2018.

[4]   H. Moustaf, A. M. Youssef, M. T. Nour, "Investigation of morphology, mechanical, thermal and flame properties of EVA/EPDM blend by combination of organoclay with Na^+-tripolyphosphate," *RSC Adv.*, vol. 6, pp. 36467–36474, 2016.

[5]   A. W. Hu, Z. H. Fu, "Nanotechnology and its application in packaging and packaging machinery," *Packaging Engineering,* vol. 24, pp. 22-24, 2003.

[6]   M. A. Nassar, A. M. Youssef, "Mechanical and antibacterial properties of recycled carton paper coated by PS/Ag nanocomposites for packaging," *Carbohydrate Polymers*, vol. 89, pp. 269–274, 2012.

[7]   A. M. Youssef, F. M. Malhat, A. Abdel Hakim, I. Dekany, "Synthesis and utilization of poly (methylmethacrylate) nanocomposites based on modified montmorillonite," *Arabian Journal of Chemistry*, vol. 10, pp. 631–642, 2017.

[8]   D. Sun, N. Miyatake, H-J. Sue, "Transparent PMMA/ ZnO nanocomposite films based on colloidal ZnO quantum dots," *Nanotechnology*, vol. 18, no. 21, pp. 215606, 2007

[9]   W. Brostow, M. Dutta, T. Ricardode Souza, P. Rusek, A. Marcos de Medeiros, E. N. Ito, "Nanocomposites of poly (methyl methacrylate) (PMMA) and montmorillonite (MMT) Brazilian clay: a tribological study," *Express PolymLett.*, vol. 4, no. 9, pp. 570–575, 2010.

[10]   J. Zheng, Q. Su, C. Wang, G. Cheng, R. Zhu, J. Shi, K. Yao, "Synthesis and biological evaluation of PMMA/MMT nanocomposite as denture base material," *J Mater Sci Mater M.*, vol. 22, no. 4, pp. 1063–1071, 2011.

[11]   F. Yang, G. L. Nelson, "PMMA/silica nanocomposite studies: synthesis and properties," *J Appl Polym Sci.*, vol. 91, no. 6, pp. 3844–3850, 2004.

[12]   H. P. Fu, R. Y. Hong, Y. J. Zhang, H. Z. Li, B. Xu, Y. Zheng, D. G. Wei, "Preparation and properties investigation of PMMA/ silica composites derived from silicic acid," *PolymAdv Technol.*, vol. 20, pp. 84–91, 2009.

[13]   A. M. Youssef, F. M. Malhat, A. A. Abdelhakim, "Preparation and Utilization of Polystyrene Nanocomposites based on TiO_2 nanowires," *Polymer-Plastics Technology and Engineering*, vol. 52, pp. 228–235, 2013.

[14]   K. Matsuyama, K, Mishima, T. Kato, K. Irie, K. Mishima, "Transparent polymeric hybrid film of ZnO nanoparticle quantum dots and PMMA with high luminescence and tunable emission color," *J Colloid Interface Sci.*, vol. 367, pp. 171–177, 2012.

[15]   H. H. El-Maghrabi, A. Barhoum, A. A. Nada, A. M. Youssef, Y. M. Moustafa, S. M. Seliman, M. Bechelany, "Synthesis of mesoporous core-shell $CdS@TiO_2$ (0D and 1D) photocatalysts for solar-driven hydrogen fuel production," *J. Photochemistry and Photobiology A: Chem.*, vol. 351, pp. 261–270, 2018.

[16]   R. Balen, W. Vidotto da Costa, J. De Lara Andrade, "Structure, thermal, optical properties and cytotoxicity of PMMA/ZnO fibres and films: potential application in tissue engineering," *Appl Surf Sci.*, vol. 385, pp. 257–267, 2016.

[17]   A. Azlovar, K. Kogej, Z. Crnjak, "Polyol mediated nanosize zinc oxide and nanocomposites with poly (methyl methacrylate)," *Polymer Letters,* vol. 5, no. 7, pp. 604-619, 2011.

[18]   I. S. Elashmawi, N. S. AIatawia, N. H. El-Sayed, "Preparation and characterization of polymer nanocomposites based on PVDF/PVC doped with graphene nanoparticles," *Results in Physics*, vol. 7, pp. 636-640, 2017.

[19]   M.I. Mohammed, "Optical properties of ZnO nanoparticles dispersed in PMMA/PVDF blend," *Journal of Molecular Structure*, vol. 1169, pp. 9-17, 2018.

[20]   M. Agrawal, A. Pich, S. Gupta, N.E. Zafeiropoulos, J.R. Retama, M. Stamm, "Temperature sensitive hybrid microgels loaded with ZnO nanoparticles," *J. Mater. Chem.*, vol. 18, pp. 2581-2586, 2008.

[21]   A M. Youssef, A. M. El-Nahrawy, A. B. AbouHammad, "Sol-gel synthesis and characterizations of hybrid chitosan-PEG/calcium silicate nanocomposite modified with ZnO-NPs and (E102) for optical and antibacterial applications," *International Journal of Biological Macromolecules*, vol. 97, pp. 561–567, 2017.

[22] J. Zheng, R. Ozisik, R. W. Siegel, "Disruption of self-assembly and altered mechanical behavior in polyurethane/zinc oxide nanocomposites," *Polymer*, vol. 46, no. 24, pp. 10873-10882, 2005.

[23] X.Y. Gao, Y.C. Zhu, S. Zhou, W. Gao, Z.C. Wang, B. Zhou, "Preparation and characterization of well-dispersed water borne polyurethane/$CaCO_3$ nanocomposites," *Colloids Surf. Colloids Surf. A Physicochem. Eng. Asp.*, vol. 377, pp. 312-317, 2011.

[24] R.Y. Hong, J.H. Li, L.L. Chen, D.Q. Liu, H.Z. Li, Y. Zheng, J. Ding, "Synthesis, surface modification and photocatalytic property of ZnO nanoparticles," *PowderTechnol.*, vol. 189, no. 3, pp. 426-432, 2009.

[25] W. Liao, A. Gu, G. Liang, L. Yuan, "New high performance transparent UV curable poly(methyl methacrylate) grafted ZnO/silicone-acrylate resin composites with simultaneously improved integrated performance," *Colloids Surf.*, vol. A 396, pp. 74-82, 2012.

[26] P. Ilangovan, M. S. Sakvai, A. B. Kottur, "Synergistic effect of functionally active methacrylate polymer and ZnO nanoparticles on optical and dielectric properties," *Mater Chem Phys.*, vol. 193, pp. 203–211, 2017.

[27] F. Wang, Y. Wen, T. Bai, "The composite hydrogels of polyvinyl alcohol–gellan gum-Ca^{2+} with improved network structure and mechanical property," *Mater. Sci. Eng. C.,* vol. 69, pp. 268-275, 2016.

[28] D. Raoufi, T. Raoufi, "The effect of heat treatment on the physical properties of sol–gel derived ZnO thin films," *Appl Surf Sci.*, vol. 255, pp. 5812–5817, 2009.

[29] E. Kandare, H. Deng, D. Wang, J. M. Hossenlopp, "Thermal stability and degradation kinetics of poly(methylmethacrylate)/layered copper hydroxy methacrylate composites," *Polym Adv Technol.*, vol. 17, no. 4, pp. 312–319, 2006.